

Simulation of the GlueX Barrel Calorimeter.

R. Hakobyan, Z. Papandreou, B. Leverington

Department of Physics, University of Regina, SK, S4S 0A2, Canada

Abstract: Detailed detector simulations of the Barrel Calorimeter and each single module have been performed. As input data for the detector simulations the output of the *genr8* phase-space distributed event generator have been used. The simulations show that the Barrel Calorimeter contains about 97% of the shower energy produced by the η and π^0 decay photons.

The energy deposited in 1cm^2 segments of the BCal module is simulated for readout purposes.

1 Introduction

The Barrel Calorimeter (BCal) resolution [1] and length [2] studies had been performed using the HDFast simulation program based upon the MCFast framework developed by the simulation group at Fermilab.

The BCal Monte Carlo simulation programs, GBCAL [3] and GBCMOD [4], are based on the GEANT 3.21 library [5,6], widely used in current high-energy and astroparticle physics experiments. The GBCMOD program is for the simulation of a single module of the Barrel Calorimeter[7-9], while the GBCAL simulates the entire Barrel Calorimeter (48 modules),

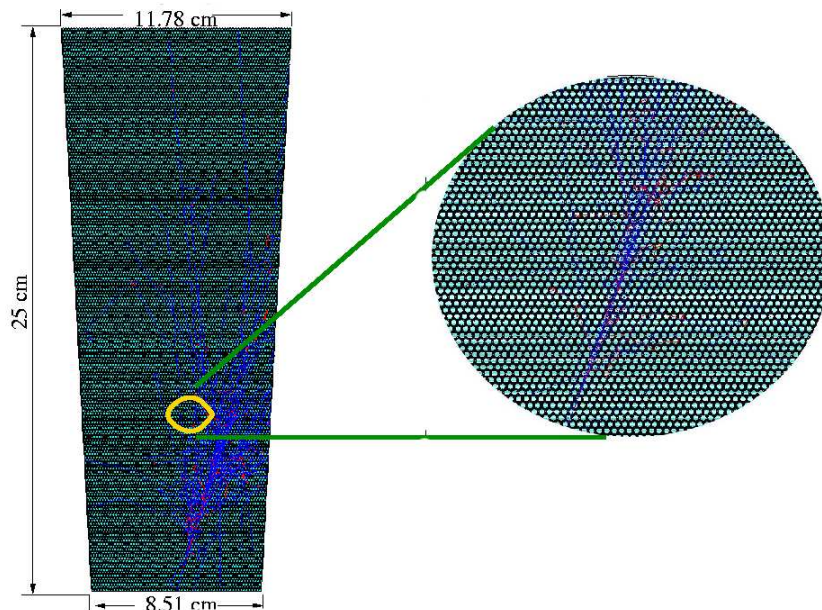


Figure 1: The Barrel Calorimeter is composed of 48 trapezoidal shaped modules with the indicated sizes.

including the Start Counter (ST), Cylindrical Drift Chamber (CDC) and target (liquid Hydrogen filled tube of 30 cm length and 4cm diameter). GBCAL incorporates a detailed description of the GlueX apparatus [9,10], and the real geometry of the BCal module that has been built by the SPARRO group at the University of Regina. The details of the BCal module geometry are presented in Sect. 2, and the outcome of the simulations is presented in Sect. 3.

2 Barrel Calorimeter

2.1 BCal module and its geometry

The BCal module with 4 m length and 25 cm thickness has a trapezoidal cross-section, with bases of 8.51 and 11.78 cm (see Figure 1). The module structure consists of a stack where alternating layers of scintillating fibers of 1mm diameter are glued inside thin grooved lead layers of 0.5 mm thickness. A piece of the module is shown in Figure 2. where the clipping clearly shows the stack of the embedded scintillating fibers. Apart from the glue rings around the scintillating fibers with a thickness of 0.05 mm, there are glue boxes between the scintillating fibers along the horizontal direction as is shown in Figure 3 (thicknesses have

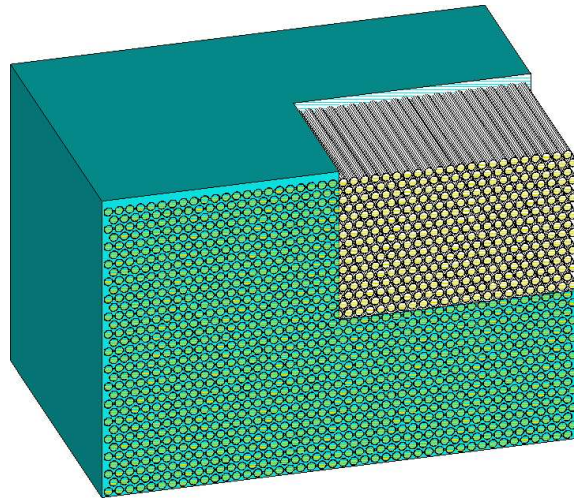


Figure 2: A piece of the BCal module where clipping clearly shows the stack of the embedded scintillating fibers.

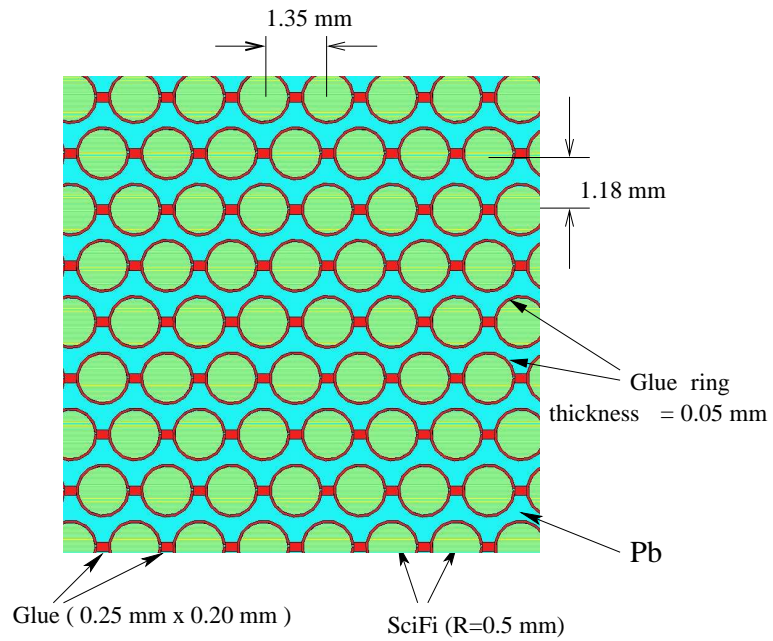


Figure 3: Inside view of the BCal module with its detailed geometry.

been measured with a microscope). These glue (BICRON-600) boxes (indicated in red in Figure 3) have $0.25 \times 0.20 \text{ mm}^2$ cross-sections and this fact is taken into consideration in our simulations. The composite has a volume ratio Pb:SciFi:Glue of 37:49:14 corresponding to a density of about 5 g/cm^3 and a radiation length X_0 of 1.5 cm [11,12]. The final stack has a depth of 25 cm corresponding to 212 planes of lead/SciFis. As it is shown in Figure 3 the horizontal and vertical distances between the centers of the fibers are 1.35 mm and 1.18 mm, respectively. Each BCal module with this geometry comprises 15640 scintillating fibers in it.

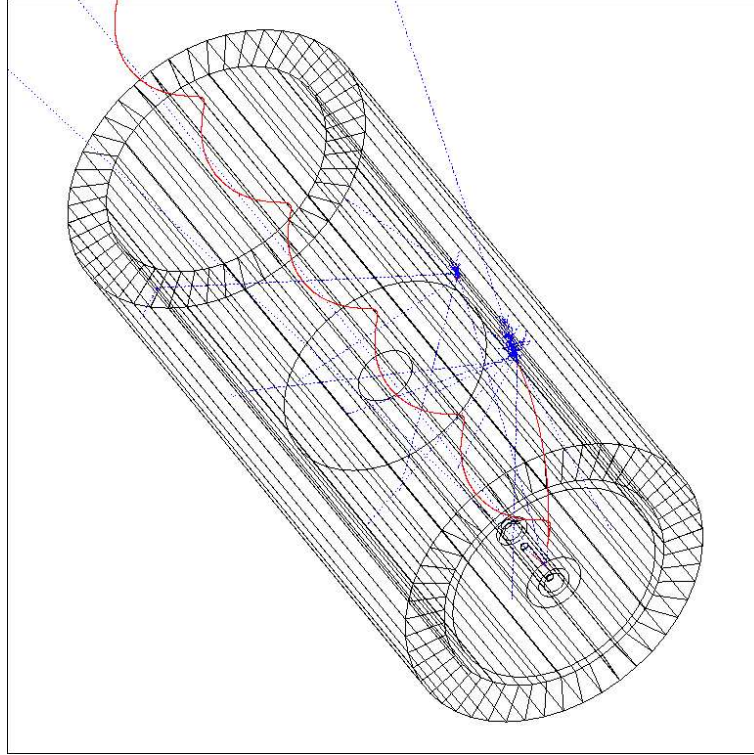


Figure 4: Transparent view of the BCal along with the target, ST and CDC.

2.2 Barrel Calorimeter

The almost cylindrical Barrel Calorimeter (Figure 4 and Figure 5) consists of 48 modules with the geometry described in the previous section. The BCal will be positioned inside the solenoid which constrains its outer radius to be 90 cm. On the other hand, the inner radius is constrained to be 65 cm in order to allow the Cylindrical¹ and Forward² Drift Chambers, Start Counter³ and target to be positioned inside of the Barrel Calorimeter.

In the GBCAL simulation code all these detectors are involved in the simulations since they can change the energy and the position of particles entering into the calorimeter.

¹The Cylindrical Drift Chamber is filled with argon gas at the temperature of 300 K and pressure of 1 atm. The existence of the straw tube wires are not considered in our simulations.

²The Forward Drift Chambers are not involved in our simulations since they provide information about the forward going particles that do not play a role in our simulations.

³The Start Counter is cylinder composed of a scintillator of 3 mm thickness and has a conical downstream end [9,10].

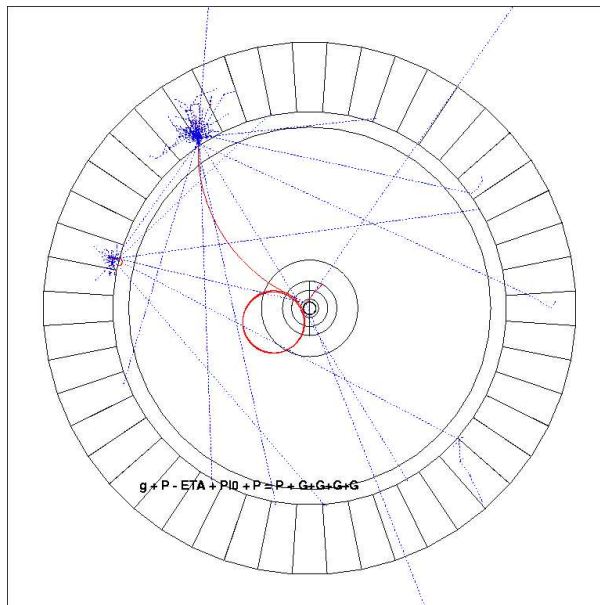


Figure 5: Front view of the BCal along with the target, ST and CDC.

Simulations have been done not only for the BCal module with the real geometry, but also for a BCal of mixed material composed of lead, scintillating fiber and glue [11] with the volume ratio of 37:49:14. In Figure 6 the calculated photon cross section in Pb-SciFi-Glue mixed material is presented for a wide range of photon energies. One can see that the pair production in the Coulomb field of the nuclear plays the dominant role in our energy range of interest.

3 The simulation results

3.1 The generated events

As an input for the detector simulation the reaction (1) is generated

$$\gamma + p \rightarrow \eta + \pi^0 + p \rightarrow (\gamma + \gamma) + (\gamma + \gamma) + p \quad (1)$$

using the *genr8* phase-space distributed event generator. The energy and angular distributions for the photons and proton are presented in Figure 7a and Figure 7b, respectively. One can see that most protons carry a comparatively small amount of the momentum and are produced mainly at large angles with respect to the beam direction giving smaller amounts of energy deposited in the lead and scintillating fibers. On the other hand, the η and π^0 decay photons are mostly forward and carry the largest part of the energy. Only the photons emitted at larger than 10 degrees can enter the BCal, and Figure 7b shows that the number of photons going forward (at less than 10 degrees) is large (about 40%). Nevertheless more than 6% of those forward going photons produce e^-e^+ pairs in the Start Counter or Cylindrical Drift Chamber environment¹, and at least one of those leptons gives a shower in the BCal as is shown in Figure 4 and Figure 5.

¹The e^-e^+ pairs are mainly produced in the Start Counter. The pair production in the CDC is negligible.

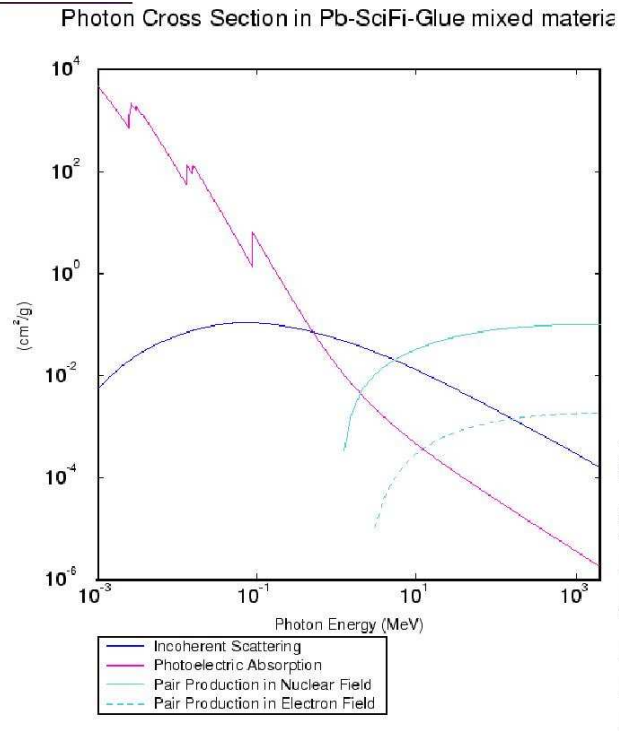


Figure 6: Calculated cross-sections for the photons passing through the Lead-SciFi-Glue mixed material of the BCal with the volume ratio of 37:49:14.

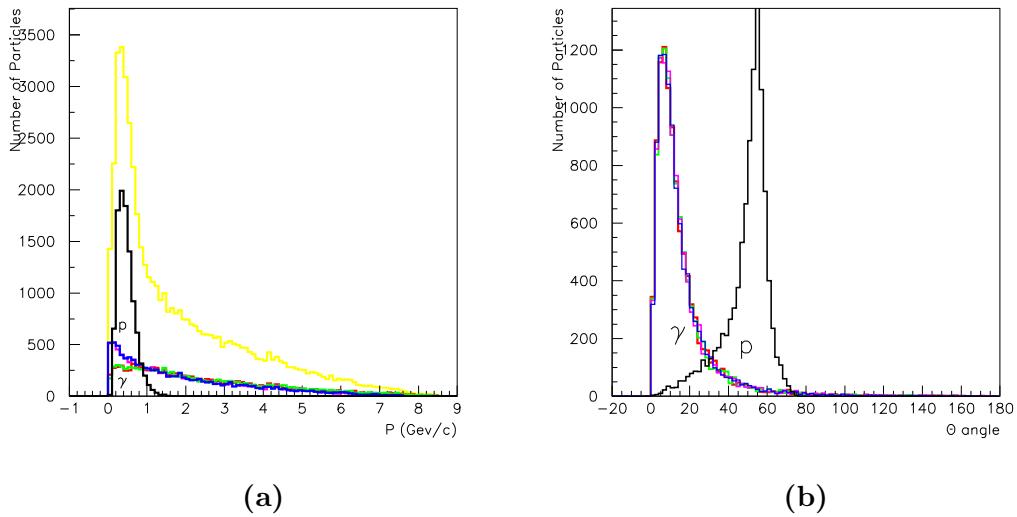


Figure 7: a) Energy distribution of the generated photons and proton produced in reaction (1). The yellow histogram is the momentum distribution of all generated particles. b) Angular distribution of particles produced in reaction (1). θ is the production angle of particles with respect to the beam direction. The black histograms represent the proton, while the color ones are for the photons.

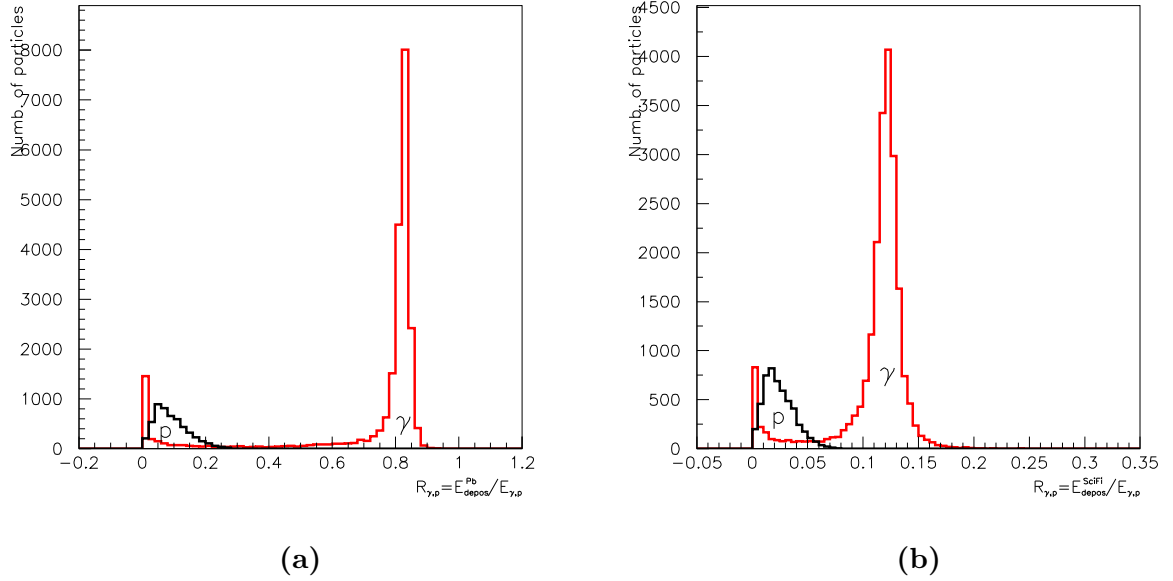


Figure 8: a) The distribution of the ratio of the deposited energy in the lead and the incident particle (photon or proton) energy. b) The distribution of the ratio of the deposited energy in the scintillating fibers and the incident particle (γ or p) energy.

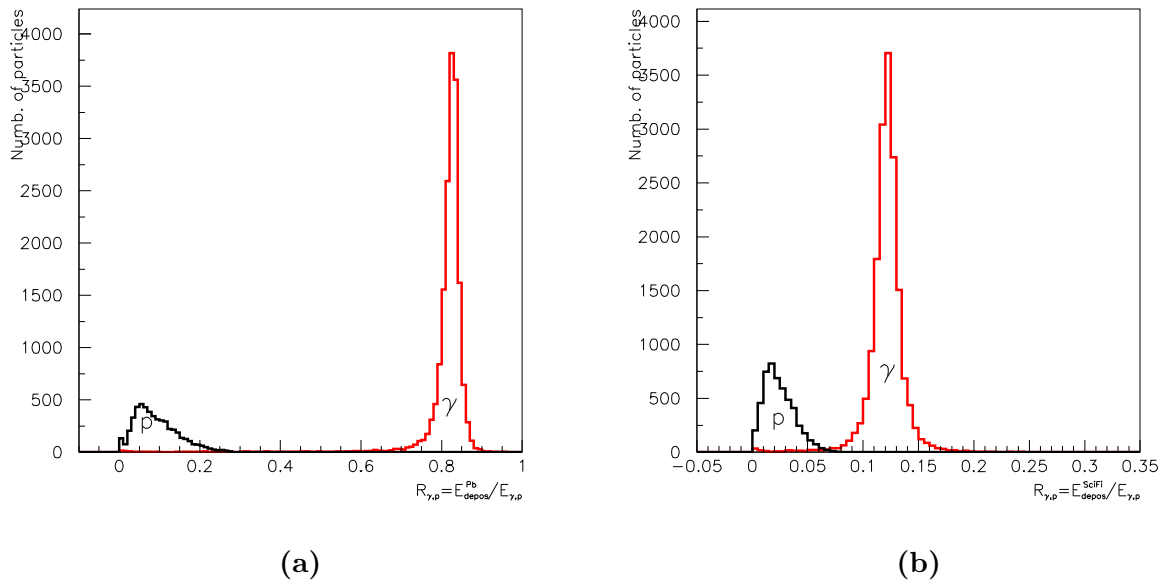


Figure 9: The same as in Figure 8 but without forward going photons that give pair production in the ST or CDC environments.

3.2 The outcome of the detector simulations

3.2.1 BCal Module

The simulation of the trapezoidal shaped single module of the BCal (GBCMOD) shows that the energies deposited in the lead, scintillating fibers and glue are respectively about 77.1%, 11.8% and 3.8% of the incident photon energy. The rest (7.3%) of the energy exits from the module, out of which about 3.5% leaks out the sides (from both sides in total). But in reality this 3.5% of the energy enters into adjacent modules and can be measured. Unfortunately there are some photons, electrons and positrons exiting from the front and back sides of the module and their energy is not recoverable. The exit of the particles from the front side (inner part of the BCal) are the results of the bent trajectories of electrons and positrons in the 2 T magnetic field, and those low energy electrons and positrons can produce a bremsstrahlung photons having a backward direction. Such photon production is presented in Figure 4 and Figure 5.

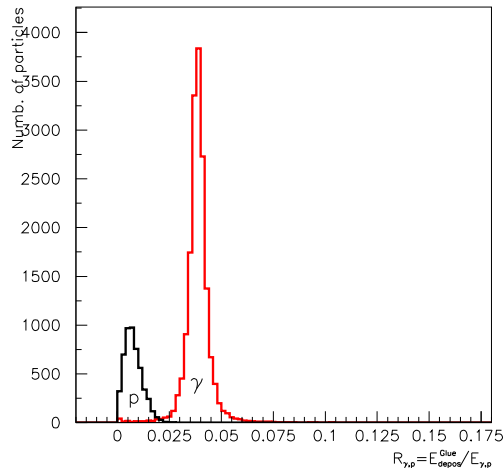


Figure 10: The distribution of the ratio of the energy deposited in the glue and the incident photon energy (proton energy).

This estimation has been obtained for the event samples where photons with fixed energies are incident at the center of the module and always perpendicular to the face of the module. This is a particular case where many more shower particles can exit from the back side of the module because of the short range of photon's path in the BCal material. Table 1 presents the mean percentage of the energies deposited in the lead, scintillating fibers and glue materials by the photons of the fixed 200, 500 and 1000 MeV energies incident on the centre of the module and perpendicular to the face.

3.2.2 Entire BCal

In reality photons rarely enter the BCal module perpendicular to the module face. In fact, they can have different momenta and will enter the module at different angles and positions. To that end 10,000 phase space distributed events are generated for the reaction (1), where photon beam energy is 9 GeV. Figure 8 presents the distribution of the ratio of the total

| E_γ (MeV) | $R_{Pb} = \frac{E_{depos}^{Pb}}{E_\gamma}$ ($R'_{Pb} = \frac{E_{depos}^{Pb}}{E_{depos}}$) | $R_{SciFi} = \frac{E_{depos}^{SciFi}}{E_\gamma}$ ($R'_{SciFi} = \frac{E_{depos}^{SciFi}}{E_{depos}}$) | $R_{Glue} = \frac{E_{depos}^{Glue}}{E_\gamma}$ ($R'_{Glue} = \frac{E_{depos}^{Glue}}{E_{depos}}$) |
|------------------|--|--|--|
| 200 | 77.4% (83.1%) | 11.9% (12.8%) | 3.8% (4.1%) |
| 500 | 77.1% (83.2%) | 11.8% (12.7%) | 3.8% (4.1%) |
| 1000 | 76.7% (83.2%) | 11.7% (12.7%) | 3.8% (4.1%) |

Table 1: The mean percentage of the energy deposited in the lead, scintillating fibers and glue of the BCal module by the photons of the fixed 200, 500 and 1000 MeV energies incident on the centre of the module and perpendicular to the face.

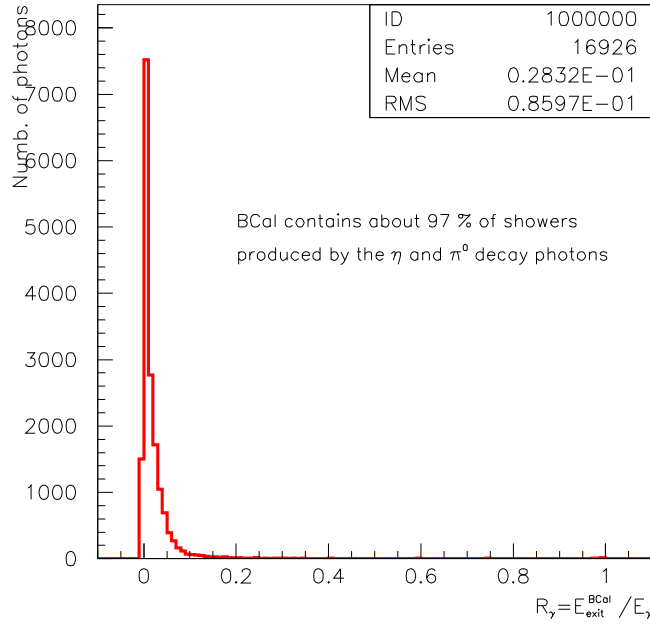


Figure 11: The distribution of the ratio of the photon produced shower particles' energy that are exited from the BCal and the energy of the incident photon.

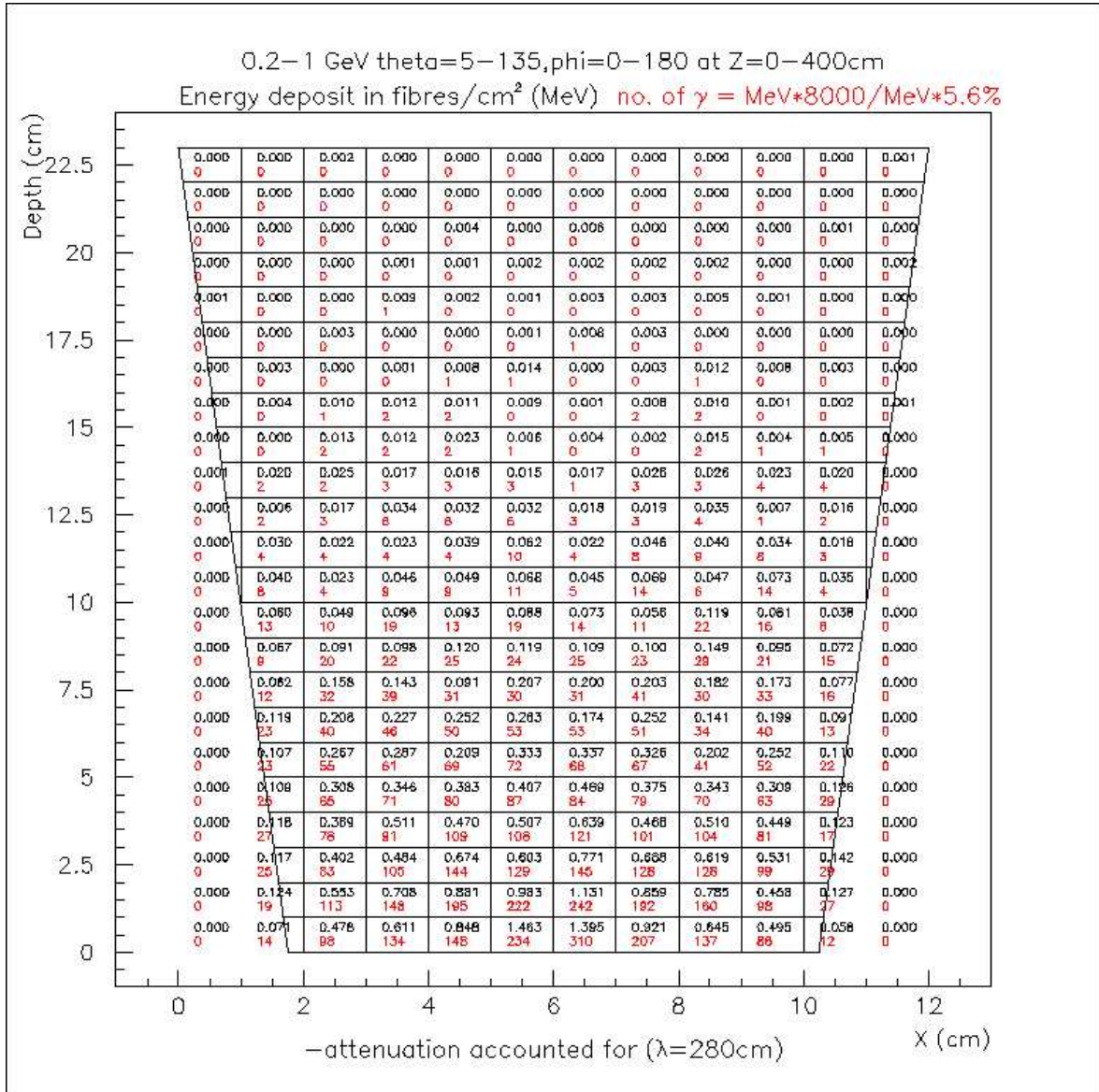


Figure 12: The table of the deposited energies and the number of photons in 1cm x 1cm segmented BCal module.

deposited energy in the lead (a) (scintillating fibers (b)) of the entire Barrel Calorimeter and the incident η and π^0 decay photon's energy.

| R_{Pb} | R_{SciFi} | R_{Glue} | R'_{Pb} | R'_{SciFi} | R'_{Glue} |
|----------|-------------|------------|-----------|--------------|-------------|
| 81.2% | 12.1% | 3.9% | 83.5% | 12.4% | 4.0% |

Table 2: The mean percentage of the energy deposited in the lead, scintillating fibers and glue of entire barrel calorimeter by the η and π^0 decay photons. The ratios are defined the same as in Table 1.

One can see that the deposited energy caused by the photons has two peaks. The peak at the low values of R ratio comes from the forward going photons ($\Theta \leq 10^0$). Those photons give pair production in the ST, and the latter can bring the small amount of energy deposited in the BCal like it is shown in Figure 4 and Figure 5.

Figures 9a and 9b are the repeated distributions of Figures 8a and 8b but without the abovementioned forward going photons that create an e^-e^+ pairs in the Start Counter.

Energy deposited in the glue material of the BCal by the photons is presented in Fig. 10. The average deposited energies that the η and π^0 decay photons leave in the lead, scintillating fibers and glue substances of the BCal are presented in Table 2.

Figure 11 shows the distribution of the photon induced shower energy that exit from the Barrel Calorimeter. This plot indicates that the Barrel Calorimeter with the given geometry contains about 97% of the energy of the shower, which compares favourably to the KLOE calorimeter's results [11,12]. This plot includes the shower particles that have exited from the inner part of the BCal giving an energy deposited in the opposite modules of the BCal (such photons are shown in Figure 4 and Figure 5).

3.2.3 The readout segmentation

For the readout purposes we are interested in the energy deposited in small segments of the BCal. To determine the final sizes of the segments for the readout purpose we have tabled the energies deposited in the scintillating fibers embedded in 1cm x 1cm x 400cm volumes.

In Figure 12 the number of photons (red figures) as well as the portion of the deposited energies in the scintillating fibers embedded in the given segments are presented. The number of photons are calculated taking into account the fibers' attenuation length ($\lambda= 280$ cm), the trapping efficiency of the scintillating fibers (5.6%) and the number of photons per MeV (~ 8000 γ/MeV) specific to this type of scintillating fibers.

4 Summary

Deposited energies are estimated in different materials (lead, scintillating fiber, glue) of the Barrel Calorimeter caused by the η and π^0 decay photons. From the single BCal module and the entire Barrel Calorimeter simulations it is shown that an average 12% of an incident photon energy will be deposited in the scintillating fibers, 81% in the lead and 4% in the glue

(BICRON-600). Detailed simulations have been performed for the readout segmentation of the module. It is shown that the first ten centimeters of the module's length contains the main part of the shower. It is shown as well that the BCal with the given geometry contains about 97% of the electromagnetic showers.

Acknowledgment

We are very thankful to George Lolos, Garth Huber and Mauricio Barbi for the useful and constructive discussions and comments.

References

- [1] G.M. Huber, BCAL Resolution study using HDFast, GlueX-doc-382-v1
- [2] G.M. Huber, BCAL Length Study using HDFast, GlueX-doc-334-v2
- [3] R. Hakobyan, The GBCAL stand-alone program for the simulation of the GlueX Barrel Calorimeter, <http://p3i.uregina.ca/?q=node/68>
- [4] R. Hakobyan, The GBCMOD program for the simulation of the BCal module, <http://p3i.uregina.ca/?q=node/42>
- [5] R.Brun, et al., GEANT3, CERN-DD/EE/84-1 (1984)
- [6] R.Brun, et.al., GEANT: Simulation program for particle physics experiments, user guide and reference manual, CERN-DD-78-2-REV (1978)
- [7] A.R. Dzierba, C.A. Meyer and E.S. Swanson, American Scientist, **88**, 406 (2000)
- [8] G.J. Lolos, Eur. Phys. **J. A17**, 499 (2002)
- [9] GlueX/Hall-D Collaboration, The Science of Quark Confinement and Gluonic Excitations, GlueX/Hall-D Design Report, Ver.4 (2002)
- [10] The GlueX Collaboration, Summaries of GlueX Detector Systems, GlueX-doc-323
- [11] Z.Papandreou, R. Hakobyan, N.Kolev, Radiation length calculation, GlueX-doc-439-v3
- [12] Z.Papandreou, BCAL for dummies, P3I Portal, <http://p3i.uregina.ca/?q=node/33>
- [13] M. Adinolfi et al., NIM A 482, 364 (2002)
- [14] M. Adinolfi et al., NIM A 494, 326 (2002)